JOURNAL OF GEOPHYSICAL RESEARCH, VOL. 104, NO. B11, PAGES 25,513–25,527, NOVEMBER 10, 1999

# Modeling dynamic recrystallization of olivine aggregates deformed in simple shear

H.-R. Wenk

Department of Geology and Geophysics, University of California, Berkeley

C. N. Tomé

Materials, Science and Technology Division, Los Alamos National Laboratory, Los Alamos, New Mexico

**Abstract.** Experiments by *Zhang and Karato* [1995] have shown that in simple shear dislocation creep of olivine at low strains, an asymmetric texture develops with a [100] maximum rotated away from the shear direction against the sense of shear. At large strain where recrystallization is pervasive, the texture pattern is symmetrical, and [100] is parallel to the shear direction. The deformation texture can be adequately modeled with a viscoplastic self-consistent polycrystal plasticity theory. This model can be expanded to include recrystallization, treating the process as a balance of boundary migration (growth of relatively underformed grains at the expense of highly deformed grains) and nucleation (strain-free nuclei replacing highly deformed grains). If nucleation dominates over growth, the model predicts a change from the asymmetric to the symmetric texture as recrystallization proceeds and stabilization in the "easy slip" orientation for the dominant (010)[100] slip system. This result is in accordance with the experiments and suggests that the most highly deformed orientation components dominate the recrystallization texture. The empirical model will be useful to simulate more adequately the development of anisotropy in the mantle where olivine is largely recrystallized.

## 1. Introduction

Simple shear experiments of rock-forming minerals and analogs deformed by dislocation creep reveal some puzzling features. After moderate strains, the deformed original grains develop a characteristically asymmetric preferred orientation pattern with a monoclinic symmetry, including a mirror plane perpendicular to the shear plane and containing the shear direction. These experimental simple shear deformation textures (in this paper the term texture is used synonymous with lattice preferred orientation), such as those for quartz [*Dell'Angelo and Tullis*, 1989], calcite [*Kunze et al*., 1998], and olivine [*Zhang and Karato*, 1995], can be predicted with polycrystal plasticity theory (for example, for calcite, *Wenk et al*. [1987], for quartz, *Wenk et al*. [1989], and for olivine *Wenk et al*. [1991]). However, in simple shear experiments at higher strains the larger original grains are replaced by fine, dynamically recrystallized grains. The texture that develops is very strong and consists of one or several symmetry-related orientation components. The observed texture reaches a steady state in terms of strength as well as pattern and does not change appreciably with increasing strain [e.g., *Pieri and Olgaard*, 1997]. Pole figures display a nearly orthorhombic symmetry that is not expected for simple shear deformation; they have additional mirror planes perpendicular to the shear direction and parallel to the shear plane. Examples include quartz [*Dell'Angelo and Tullis*, 1989], olivine [*Zhang and Karato*, 1995], norcamphor, a quartz analog [*Herwegh and Handy*, 1996], ice [*Duval*, 1981; *Bouchez and Duval*, 1982; *Burg et al*., 1986], and calcite [*Pieri and Olgaard*, 1997; *Kunze et al*., 1998], all materials with low crystal symmetry.

These orthorhombic textures cannot be predicted with polycrystal plasticity theory for deformation by dislocation glide such as Taylor, Sachs, or self-consistent models. Authors have referred to the textures as "easy slip" orientations [e.g., *Schmid and Casey*, 1986], implying that a microscopic slip plane of an active slip system is parallel to the macroscopic shear plane and a microscopic slip direction is parallel to the shear direction, and therefore deformation on such a slip system in simple shear is "easy." So far, there has been no explanation to how crystals rotate and remain within those orientations. *Herwegh and Handy* [1996] suggest a "rigid body rotation" into the easy slip orientation and an unexplained cessation of rotation once those special orientations are reached.

Experimental textures that display this easy slip component have been produced in a simple shear geometry, and the corresponding microstructures are indicative of complete dynamic recrystallization and grain size reduction. Similar textures have been observed in naturally deformed rocks from the Earth's crust and mantle, where recrystallization is prevalent. In order to simulate the deformation in the Earth it is therefore necessary to have a reliable model that considers not only deformation but also recrystallization. *Jessell* [1988] proposed a model for fabric development during dynamic recrystallization using the Taylor theory. In this study we refine a deformation-based recrystallization model [*Wenk et al*., 1997] that relies on the viscoplastic self-consistent theory and apply it to the problem of simple shear deformation of olivine. The model is not intended to explain detailed mechanisms of recrystallization, but rather it uses general concepts about dynamic recrystallization to explain the evolution of texture and anisotropy.

Olivine is of great geophysical importance because it is the



Paper number 1999JB900261.
0148-0227/99/1999JB900261$09.00

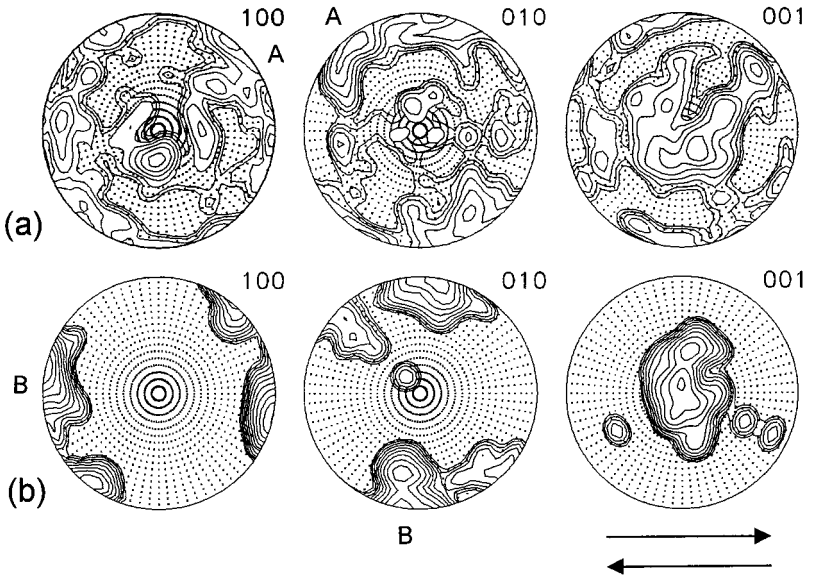


**Figure 1.** Pole figures of experimentally deformed olivine from *Zhang and Karato* [1995] (a) Specimen PI-148 with a deformation microstructure of original grains without recrystallization, $\varepsilon = 17\%$, 1473 K. (b) Specimen PI-150 with dynamic recrystallization by boundary migration, $\varepsilon = 150\%$, 1573 K. U-stage data have been entered into orientation distribution function (ODF) and were then smoothed with 15° Gaussians. Double arrows in this and the following figures indicate the shear direction and the sense of shear. Projections are equal-area; logarithmic contours are 0.5, 0.7, 1.0, 1.4, 2 multiples of a random distribution (mrd), etc.; dot pattern is below 1 mrd.

major constituent of the Earth's upper mantle. Olivine rocks such as peridotite deform and develop preferred orientation during convection, and the resulting crystal alignment is the cause of seismic anisotropy [e.g., *Silver*, 1996]. Most of the upper mantle peridotites that are collected on the Earth's surface show microstructures indicative of recrystallization [*Ben Ismail and Mainprice*, 1998; *Mercier*, 1985; *Nicolas et al*., 1971; *Nicolas et al*., 1973; *Skrotzki et al*., 1990]. Therefore recrystallization processes of olivine have received a lot of attention [*Avé Lallemant and Carter*, 1970; *Karato*, 1988; *Karato et al*., 1980; *Toriumi and Karato*, 1985]. In order to be able to model the development of anisotropy during mantle convection realistically, it is important to develop a better understanding of how dynamic recrystallization modifies the lattice preferred orientation of olivine. Good comparisons for a simulation study are provided by simple shear experiments of *Zhang and Karato* [1995] that show a transition from deformed original grains to recrystallized grains. During deformation, original grains develop an asymmetric concentration of [100] axes, displaced about 30° from the shear direction against the sense of shear (component A) [*Zhang and Karato*, 1995] (Figure 1a). At larger strains, with greater degree of recrystallization, component A disappears and is replaced by component B with [100] in the shear direction and poles to (010) parallel to the shear plane normal (Figure 1b).

We will first discuss deformation models, then introduce the features of a deformation-based model for dynamic recrystallization, and apply this model to predict texture and microstructure development of olivine deformed in simple shear to large strains where dynamic recrystallization is complete.

## 2. Model

Several models based on polycrystal plasticity theory have been developed to predict the deformation behavior of a polycrystal by mechanisms such as dislocation glide, mechanical twinning, and, more recently, dynamic recrystallization [e.g., *Lebensohn et al*., 1998]. Each of these models captures some important features of a material and particular deformation mechanisms, but none is universal, and a model may be more or less suitable for a specific system. As with all models, reasonable judgement needs to be exercised in recognizing their limitations. For example, the evolution of texture with progressive strain can be predicted in many cases quite satisfactorily [*Kocks et al*., 1998]. Predictions of flow stress are much less reliable, in part because the latter depend on local dislocation interactions, which are more uncertain and often influenced by impurities. In addition, the work hardening behavior is not usually known when different crystallographic systems interact. The model that we use is empirical but contains the physics of basic processes that are active during recrystallization, specifically nucleation and boundary migration. The model that we discuss in this paper is not microstructural and has no information about topology, neighbor interaction, and local heterogeneity. It treats each crystal as an inclusion in an average medium. While the specific information is therefore limited, useful results have been obtained that are pertinent to the development of preferred orientation during deformation and recrystallization. We emphasize in this paper the evolution of texture, which is most pertinent for interpreting seismic anisotropy.

### 2.1. Deformation

A real polycrystal that deforms by dislocation glide and remains coherent has to maintain strain compatibility across grain boundaries as well as stress equilibrium. From a mechanical point of view, there is a unique solution; however, the analytical solution of this problem is very difficult and requires heterogeneity inside each grain. Computer intensive finite element methods (FEM) are most appropriate to approach this

problem numerically and have been applied to a few examples [e.g., *Dawson and Beaudoin*, 1998]. In many cases simpler approximations that treat each crystal as a homogeneous unit are adequate, and two extreme sets of assumptions have been used. One approach assumes that each crystal deforms as an isolated grain in a uniform stress field without knowledge about its neighbors [*Sachs*, 1928]. The second approach assumes that each grain is completely controlled by its neighbors and undergoes the same strain as that of the aggregate, irrespective of orientation; this guarantees compatibility across grain boundaries [*Taylor*, 1938]. More recently, self-consistent models have been introduced that find an intermediate solution and satisfy stress equilibrium and strain compatibility in an average way [*Molinari et al*., 1987; *Lebensohn and Tomé*, 1993]. (There are other models, not based on polycrystal plasticity, that use continuum mechanics. The latter are questionable for aggregates of crystals deforming on discrete slip systems, and we are not going to discuss them in this paper.)

Most deformation models consider a component crystal (or grain) as a homogeneous unit. In Taylor-type models where deformation of all grains is uniform, an arbitrary deformation of a grain requires activation of up to five slip systems ("degrees of freedom"). This may require activation of unfavorably oriented systems or, if several slip modes occur, of those modes with a higher critical shear stress. Flow stresses are therefore high and Taylor-type models are known as "upper bound" models [e.g., *Kocks*, 1998].

By contrast, Sachs-type models assume that when a stress is applied to a polycrystal, the grain with the most favorably oriented slip system deforms first, independent of its neighbors. In such a model, differently oriented grains undergo different degrees of deformations, contact is not maintained across grain boundaries, and the flow stress is minimal. Thus these are "lower bound" models; strain compatibility is violated, but stress equilibrium is satisfied.

If many equivalent slip systems are available (usually in materials of high crystal symmetry) or, in the case of several slip modes, if the different modes have a similar critical shear stress, then the difference between upper and lower bound simulations is small. This is the case for rolling of fcc metals. However, in materials of low crystal symmetry and few slip systems, there can be large differences between the upper and lower bounds, and the assumption of homogeneous deformation is questionable. In these cases a viscoplastic self-consistent model has proven to be very useful for many mineral systems (for a review, see *Wenk* [1998, 1999]). In the context of dynamic recrystallization this model is particularly interesting because it predicts differences in the degree of deformation for different orientations. We have used such a model in this study. There is also experimental evidence that an assumption of lower bounds is more appropriate for minerals. For experimentally deformed olivine aggregates, *Karato and Lee* [1999] documented that grains favorably oriented for slip have higher dislocation densities.

The viscoplastic self-consistent model considers each crystal as an inclusion in a homogeneous but anisotropic medium (in the sense of *Eshelby* [1957]) whose properties are given by the average over all crystals. This inclusion then deforms, maintaining compatibility and equilibrium with the enclosing "equivalent medium." However, orientation correlation effects between grains are not accounted for by the model, and local compatibility is not maintained. Under the externally imposed deformation, favorably oriented grains deform more than others, while unfavorably oriented grains deform less. The aggregate flow stress is lower than that in a Taylor model. The formalism of the viscoplastic self-consistent theory has been described in several publications, and the reader is referred to those for details [e.g., *Molinari et al*., 1987; *Lebensohn and Tomé*, 1993, 1994; *Tomé and Canova*, 1998]. Figure 2 displays the main steps involved in the self-consistent calculation.

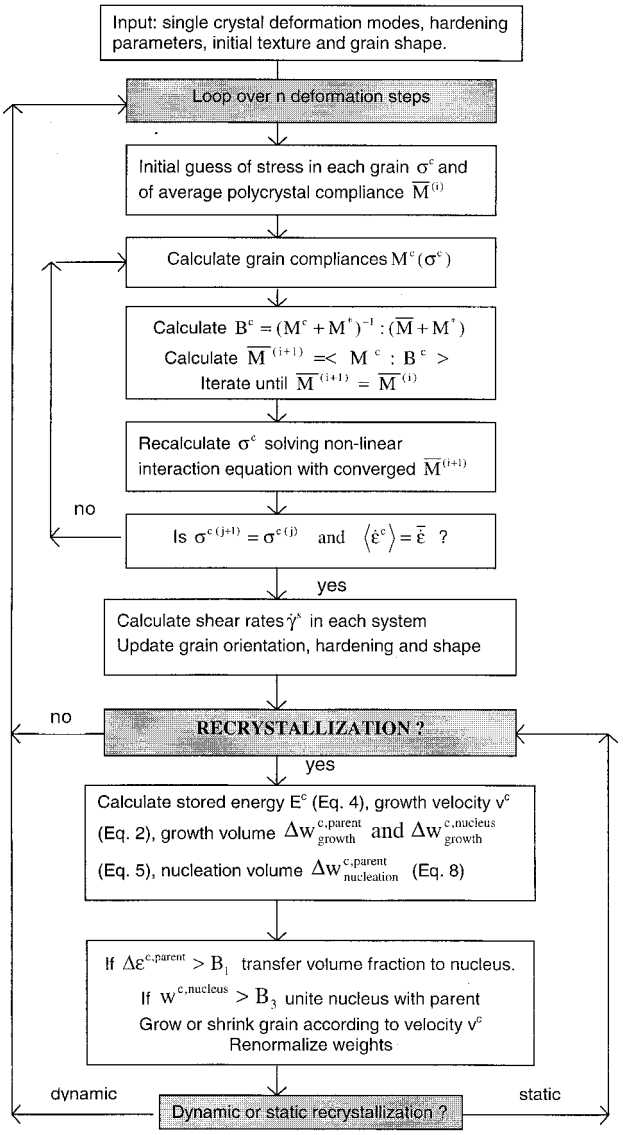


**Figure 2.** Flow diagram illustrating schematically the procedures in the viscoplastic self-consistent code, modified for recrystallization.

As a crystal deforms by slip in the self-consistent framework it undergoes a lattice rotation. This rotation has three different components. The first component is due to the macroscopic (rigid body) rotation of the sample. The second component is due to slip (plastic spin) and can be derived from the shears on the various slip systems. A crystal deforms by slip to a new shape, but it needs to rotate to fit into the provided inclusion space. The third component is due to grain morphology and applies to nonequiaxed crystals: for example, a platelet will tend to become oriented perpendicular to the compression direction. These three contributions to lattice rotation are the

**Table 1.** Critical Shear Stresses, Hardening, and Rate Sensitivity Parameters for Olivine Used in This Work

| | $\tau_0$ (I) 1-2-2-2 | $\tau_0$ (II) 1-1-2-2 | $\tau_0$ (III) 1-1-1-2 | $h$ | $n$ |
|---|---|---|---|---|---|
| (010)[100] | 1 | 1 | 1 | 0.1 | 4 |
| (001)[100] | 2 | 1 | 1 | 0.1 | 4 |
| (100)[001] | 2 | 2 | 1 | 0.1 | 4 |
| (010)[001] | 2 | 2 | 2 | 0.1 | 4 |
| (110)[001]* | 8 | 8 | 8 | 0.1 | 4 |
| (100)[011]* | 30 | 30 | 30 | 0.1 | 4 |
| (111)[101]* | 50 | 50 | 50 | 0.1 | 4 |

*Only used for numerical stability, not significantly activated.

cause of development of preferred orientations in aggregates with many component crystals.

All polycrystal plasticity models (Taylor, Sachs, and self-consistent) deal with a highly nonlinear system. A solution is obtained by working with a finite number of discrete grains (given as orientations), and deformation is applied in increments. The deformation is defined by a displacement gradient tensor that may be constant (as in this study) or may change with deformation (e.g., along a streamline during convection). In the code the rotations of all grains are calculated after each strain increment, and the orientations are then updated. In this paper the nonrandom orientation pattern that evolves is represented as pole figures, either as distributions of individual grains (sometimes with attributes to express volume fraction or nucleation events) or as maps with contours of equal pole density.

Potential slip systems need to be defined in terms of the slip plane (hkl), slip direction [uvw], critical resolved shear stress $\tau$, strain rate sensitivity (stress exponent $n$), and the hardening law. Values used for the olivine simulations are given in Table 1. They have been estimated from deformation experiments on single crystals [e.g., *Kohlstedt and Goetze*, 1974; *Bai et al*., 1991; *Hanson and Spetzler*, 1994] and cover a wide range to explore how much the model depends on detailed assumptions.

Hardening, i.e., the increase in critical shear stress because of the increase in dislocation density with strain, has contributions from "self" hardening due to dislocation interactions on each active system and "latent" hardening due to interactions of dislocations on an active system on other systems. In addition, the critical shear stress of a grain is influenced by recovery and cell formation processes. A precise local description of the microstructure and its evolution is beyond the aim of this work, and therefore we assume isotropic hardening, i.e., hardening coefficients $h^s$ for self and latent hardening are the same. Furthermore, we apply a linear hardening law, i.e., critical shear stresses $\tau$ increase linearly with strain $\gamma^s$. Since the hardening coefficients for all slip systems are assumed to be the same, the critical shear stress after a finite deformation becomes a simple function of the accumulated shear in the grain $\Gamma$:

$$\tau^s(\Gamma) = \tau_0^s(1 + \sum h^{ss'}\gamma^{s'}) = \tau_0^s(1 + h\Gamma). \quad (1)$$

If the hardening rate diminishes with strain, a more complicated hardening law could be used [*Kocks*, 1976, 1998], but as the effect of hardening on texture development is minimal, we give only results for linear hardening.

### 2.2. Recrystallization

While the reorientation associated with deformation can be adequately modeled with polycrystal plasticity theory, there is no general model for dynamic recrystallization. It is observed that more highly deformed grains accumulate larger numbers of dislocations and thus have a higher strain energy than less deformed grains [*Doherty*, 1997; *Haessner*, 1978; *Humphreys and Hatherly*, 1995]. Consequently, less deformed grains may grow through boundary migration at the expense of more deformed grains. Alternatively, dislocation-free nuclei may form in highly deformed grains, e.g., as a bulge in a grain boundary or a sufficiently misoriented subgrain, and then grow at the expense of other grains. Recrystallization is controlled by local microstructural heterogeneities, rather than "macroscopic stress and strain". However, since these heterogeneities (such as shear zones, dislocation tangles, misoriented subgrains, grain boundaries) generally increase in number and degree with deformation, the overall grain deformation provides a bulk criterion to control the recrystallization process in the model. If growth is controlling, "hard" grains with little deformation dominate the texture and highly deformed grains will disappear. If nucleation is prevalent, "soft" grains develop nuclei that will ultimately grow and dominate the fabric.

The model was originally applied to recrystallization of halite [*Wenk et al*., 1997] and has since been used to explain texture features in recrystallized calcite [*Lebensohn et al*., 1998; *Kunze et al*., 1998] and quartz [*Takeshita et al*., 1999]. The model used in this paper differs slightly from the original version as explained below.

The basic premise of the model is very simple: as a polycrystal deforms, grains favorably oriented for slip ("soft grains") deform more and accumulate dislocations. Soft grains are therefore less stable and may be consumed by less deformed grains through grain boundary migration. They are also likely to form new nuclei which then grow. The microstructure and the final texture that develop during dynamic recrystallization are a balance between nucleation and growth. The viscoplastic self-consistent theory is used to determine the deformation state of individual grains in different orientations.

*Hirth and Tullis* [1992] have identified three regimes of dislocation creep involving different mechanisms of dynamic recrystallization for quartz aggregates. With increasing temperature and decreasing strain rate the mechanisms change from (1) strain induced boundary migration to (2) progressive subgrain rotation and (3) subgrain rotation with rapid grain growth. Similar features have been observed in other mineral systems [e.g., *Urai et al*., 1986; *Karato*, 1988]. In the terminology of our model boundary, migration corresponds to growth and is controlled by the difference in strain energy between adjacent grains. The microstructure that develops by this mechanism is generally characterized by an increase in grain size. When climb is pervasive, recovery produces subgrains, separated by low-angle boundaries. During deformation, misorientations between subgrains increase. In metals, misorientations rarely exceed 2°–5° [*Engler*, 1996], and this is not sufficient to form a nucleus that grows. In anisotropic minerals, misorientations may be considerably larger so that some subgrains have sufficient misorientations to become active nuclei. This "subgrain rotation recrystallization" [*Guillopé and Poirier*, 1979; *Poirier and Guillopé*, 1979] is equivalent to nucleation in our model, though there can be other mechanisms to create nuclei.

The microstructure consists of small grains, first along boundaries and ultimately replacing all original grains.

In our model, recrystallization is allowed after the polycrystal has reached a certain amount of bulk strain which can be specified. Growth and nucleation are defined by several parameters, which are described below. It must be emphasized again that at this point the model is largely empirical but plausibly captures some of the physical mechanisms that occur during recrystallization. It relies on average properties, rather than on the real local features of the microstructure. The model is not scaled with respect to grain size or subgrain size, and the sizes enter through the empirical constants. We plan to refine the model in the future by using an N-site self-consistent deformation model that includes grain morphology [*Canova et al*., 1992; *Solas et al*., 1999] or a FEM approach [*Dawson and Beaudoin*, 1998].

### 2.3. Growth

The boundary migration rate is controlled by a growth parameter $C$. The linear growth velocity $v$ is proportional to the difference in strain energy between adjacent grains $\Delta E^{\text{stored}}$. Since the topology of the microstructure is not known, we cannot determine in which direction a boundary moves between specific neighbors. Therefore we compare the strain energy of each grain $E^c$ with the "average" $E^{\text{average}}$. If it is smaller than the weighted average, a grain grows; if it is larger, it shrinks. If it reaches some defined minimal size $C_{\text{min}}$, it disappears, i.e., the associated volume fractions are set to zero:

$$v^c = C\Delta E^{\text{stored}} = C(E^c - E^{\text{average}}). \tag{2}$$

While it is generally agreed that the stored energy drives grain boundary migration, it is less clear how to determine the stored energy. A general rule of thumb for metals is that 15% of plastic work $\Delta E^{\text{plastic}} = \Sigma \tau^s \Delta\gamma^s$ ($\Delta\gamma^s$ is the shear increment in the slip system $s$) is stored energy [*Loretto et al*., 1964, 1965; *Hirth and Lothe*, 1982]. The latter criterion, however, is incompatible with steady state flow, which corresponds to increasing plastic work without an increase in the dislocation density. From a more basic perspective it is safer to regard the stored energy as being proportional to the dislocation density $\rho$, which is in turn proportional to the square of the flow stress $\tau$,

$$E^{\text{stored}} = \rho(\mu b^2)/2 \propto \tau^2, \tag{3}$$

where $\mu$ is the shear modulus and $b$ is the Burgers vector. Dislocations occur as free dislocations in subgrain boundaries and in grain boundaries. These complexities cannot be addressed with an effective medium model that does not contain information about local heterogeneities. The details are buried in the empirical constant $C$. We assume that in the initial state all grains have zero energy and that the strain energy of the original grains is due to the work hardening component of the flow stress. Therefore we can determine the accumulated strain energy in a grain as the sum over all slip systems $s$:

$$E^c = E_0 \sum (\tau^s - \tau_0^s)^2, \tag{4}$$

where $E_0$ is a normalization factor to give units of energy, $\tau_0^s$ is the initial threshold in the absence of dislocations, and the sum is over all slip systems. Boundary migration with a linear velocity results in a change of the grain's volume fraction $w^c$:

$$\Delta w^c_{\text{growth}} = v\Delta t w^{c\,2/3} = C(E^{\text{average}} - E^c)\Delta t w^{c\,2/3}, \tag{5}$$

where $\Delta t$ is the time increment and $w$ is the original volume fraction. Implicit in the derivation is the assumption of growth or shrinkage of a sphere at a velocity $v$. Volume fractions are renormalized after each step so that the total volume fraction remains constant.

As has been noted above, the bulk dislocation density may not be too meaningful for describing boundary migration. Only dislocations close to grain boundaries really influence boundary migration. Also, it has been observed in several systems of rock analogs that newly nucleated grains grow faster than original grains, even if the latter are barely deformed [*Drury and Urai*, 1990; *Urai et al*., 1986]. This difference may reflect differences in the organization of dislocations, in surface energy, or in the number of point defects or inclusions. In the model we have introduced two growth parameters, $C^{\text{old}}$ for original grains and $C^{\text{new}}$ for new grains that have nucleated. The shrinking parameter is the weighted average of the two. In the model for olivine the two growth parameters and therefore the shrinking parameter are all equal.

### 2.4. Nucleation

Nucleation is less understood than boundary migration. It is heterogeneous and depends on local structures such as shear bands, twins, or particles. At low temperature (cold working) the increase in dislocation density due to hardening and the corresponding increase in shear stress may primarily control nucleation events. In this case the accumulated stored energy or the flow stress could provide a criterion to control nucleation, and we have used this in the previous model [*Wenk et al*., 1997]. At high temperatures, deformation reaches a steady state with no continued hardening. Recovery produces a subgrain structure, and particularly in minerals it has been observed that the subgrains become increasingly misoriented with strain (subgrain rotation recrystallization). If misorientations are large enough, subgrain boundaries become mobile, and some subgrains act as nuclei that can grow. In this case, nucleation depends on local strain increments that must be large enough to produce misorientations. An equivalent strain increment, given by the equivalent strain rate of a grain times $\Delta t$ of the step, is the criterion we use in the present study to control nucleation. In the computer code the user also has a choice to select between a stress or a strain rate criterion.

In the original recrystallization model [*Wenk et al*., 1997], nucleation was assigned a probability

$$P = \exp(-A/E^{\text{accum}})^2. \tag{6}$$

This probability was related to the accumulated strain energy, and when it exceeded the outcome (between 0 and 1) of a random number generator, nucleation took place. The nucleus entirely replaced the old grain, becoming strain-free and assuming its orientation. For a large value of the nucleation constant $A$, nucleation is unlikely.

In the modified model we are instead using a continuous nucleation rate. For a steady state the number $\Delta N$ of nuclei produced in a time period $\Delta t$ is proportional to the strain increment or, equivalently, the nucleation rate is proportional to the strain rate

$$I = dN/dt = B(\sigma, T)(d\varepsilon/dt), \tag{7}$$

where $B$ is an unknown function of stress and temperature. In our model we introduce such mechanism as follows: we assume that the volume fraction of the grain that nucleates is proportional to the nucleation rate, times the time increment:

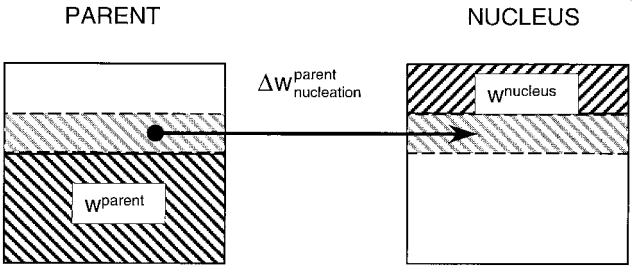


**Figure 3.** In the calculation, each grain is divided into two parts, a parent and a nucleus, with different weights. The sum of the two weights is unity. If nucleation occurs, weight is transferred from the parent to the nucleus. The parent changes its shape and critical shear stresses. The nucleus does not harden and has a spherical shape. When a threshold is reached, the nucleus is transferred back into the parent and deforms accordingly. Parent and nucleus have the same orientation.

$$\Delta w^c_{\text{nucleation}} = B\dot{\varepsilon}^c \Delta t w^c, \tag{8}$$

where $w^c$ is the current volume fraction of the grain, $\dot{\varepsilon}^c$ is its equivalent deformation rate during the incremental deformation step, and we assume that the function $B(\sigma, T)$ is a constant and give it a value $B_2$.

The general scheme is as follows: the volume fraction of each grain (with a given orientation) is partitioned into a "parent" and a "nucleated" part, such that $w^c = w^{c,\text{parent}} + w^{c,\text{nucleus}}$ (Figure 3). Initially, all the volume fraction is assigned to the parent, but it becomes modified by growth, shrinking, and nucleation. The volume fraction of the "nucleus" is initially zero but increases as nucleation proceeds. Nucleation takes place in a grain if the strain increment exceeds a specified threshold value, which is a percentage $B_1$ of the maximum strain increment in all grains. At that point, volume (i.e., weight) is transferred from the parent grain to the nucleus according to (8) (see also Figure 3). The nucleus has the same orientation as the parent but is strain-free (initial critical shear stresses), assumes initial shape (spherical), and does not harden. Both, nucleus and parent grain, grow or shrink according to growth criteria discussed in section 2.3. The nucleus generally grows faster because, since it does not harden, its accumulated energy is null. In consecutive deformation steps, nucleation (and weight transfers) may continue. When the nucleus has grown to a certain size ($B_3$, relative to the parent grain) it combines with the parent, that is, its volume is transferred back into the parent cell where the grain deforms and hardens accordingly. These transfers may occur several times. With such a scheme the total effective number of "grains" is twice as large as the number of orientations but remains constant, even though some grains may have zero weight. This simplifies the numerical procedure greatly.

Each grain in the model is characterized by an orientation, a volume fraction, a grain shape, and critical resolved shear stresses of slip systems. The volume fraction is not to be confused with the grain size. For example, an original grain that divides into subgrains of similar orientations will be represented as a single grain in the model. Also, for now, we assume that "nuclei" have the same orientation as the host which is not true in the case of subgrain rotation where nuclei show some dispersion of orientations. Such a dispersion would attenuate texture development slightly.

In the computer program we use three parameters to describe nucleation. Nucleation is allowed if an individual grain has reached a deformation threshold $B_1$. The fraction of the parent that is transferred to the nucleus in a deformation step is also prescribed ($B_2$), and the relative size of the new grain beyond which it combines with the parent grain is yet another parameter ($B_3$). The most critical parameter is $B_1$.

Using the strain rate (or strain increment) as a criterion for nucleation not only conforms to kinematic considerations of high-temperature creep but also to microstructural arguments. Nuclei may form in dislocation tangles, at boundaries with high misorientations, at mechanical twins, etc. All these microstructures are characteristic of high local deformation. In a general way, flow stress, strain, and strain increment are all related in a similar way to orientations and slip systems, though this relationship is not linear and not simple. Therefore the results from using either one of these three criteria are qualitatively similar but quantitatively not identical.

In summary, the computer program for polycrystal plasticity, augmented to include dynamic or static recrystallization, works as follows (see Figure 2): Input data are a set of initial orientations, slip systems and their critical shear stresses, and the deformation history prescribed by an incremental displacement gradient tensor. The program first performs for each step and each grain a self-consistent deformation. In case of recrystallization this is followed by growth and nucleation. At the end of each step, orientations, grain shapes, volume fractions, and critical shear stresses are updated, and the program proceeds with the next step. For static recrystallization the deformation step is omitted.

## 3. Results for Olivine

There have been several studies that simulate development of texture in olivine during deformation. Olivine, with its low orthorhombic symmetry, has only limited slip systems, and the Taylor model is therefore not directly applicable. *Takeshita et al*. [1990] have used a relaxed Taylor model in which some strain components are assumed to be accommodated by diffusion (climb). Several studies have applied various versions of the self-consistent model [*Wenk et al*., 1991; *Tommasi et al*., 1997], *Chastel et al*. [1993] used the lower bounds model, and *Parks and Ahzi* [1990] used a related hybrid model. All these simulations arrive at similar texture results with minor variations, mainly due to differences in assumed critical shear stresses for slip systems.

In this study we use three sets of critical shear stresses (Table 1). In set I (which we call 1-2-2-2 denominating CRSS ratios of the slip systems), (010)[100] slip dominates; in set II (labeled 1-1-2-2), (010)[100] slip and (001)[100] slip are equally active (approaching a pencil glide condition); and in set III (labeled 1-1-1-2), three slip systems are equally active: (010)[100], (001)[100], and (100)[001]. As we will document, the results for all three combinations are similar, indicating that as far as texture development is concerned, the model is robust and not very sensitive to exact choice of critical shear stresses. Linear hardening with a hardening coefficient $h = 0.1$ is applied and the stress exponent $n = 4$. The strain increment per step is 2%; 500 initially random orientations with the same volume fraction are used.

In this study, using the most recent version of the one-site viscoplastic self-consistent (VPSC) code (*Lebensohn and Tomé* [1993], with minor modifications), we obtain at 60% ($\gamma = 1.0$) shear deformation a texture with characteristic asymmetric

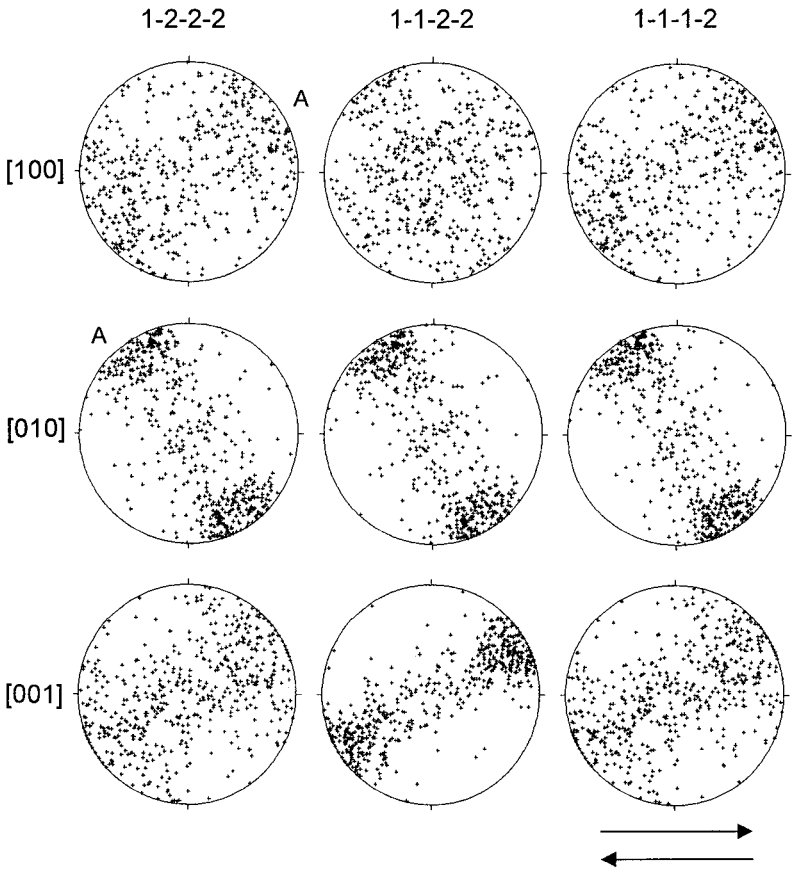


**Figure 4.** Deformation textures for olivine simulated with the one-site self-consistent polycrystal plasticity code for critical shear stress sets 1-2-2-2, 1-1-2-2, and 1-1-1-2 (Table 1). Pole figures are after 60% equivalent strain ($\gamma = 1.0$), with 500 grains; projections are equal-area.

maxima in (100) and (010) pole figures, displaced about 30° against the sense of shear (Figure 4). For 1-2-2-2 conditions, texture development is somewhat slower than for 1-1-2-2 and 1-1-1-2. The observed maximum agrees well with component *A* (Figure 1a) in the experiments of *Zhang and Karato* [1995]. With increasing strain this maximum does not rotate appreciably and corresponds to orientations where rotation rates are smallest.

In this deformation texture there are hard and soft orientations, depending on the orientations of slip systems relative to the applied stress, and this has a direct effect on the strain rate. Figure 5 shows with symbol sizes on [100] pole figures the equivalent strain rate after 40% deformation. The equivalent strain rate ranges from 0 for hard orientations (small symbols) to 0.05 for soft orientations (large symbols) in arbitrary units. In Figures 5a–5c we see extremely slow strain rates in the

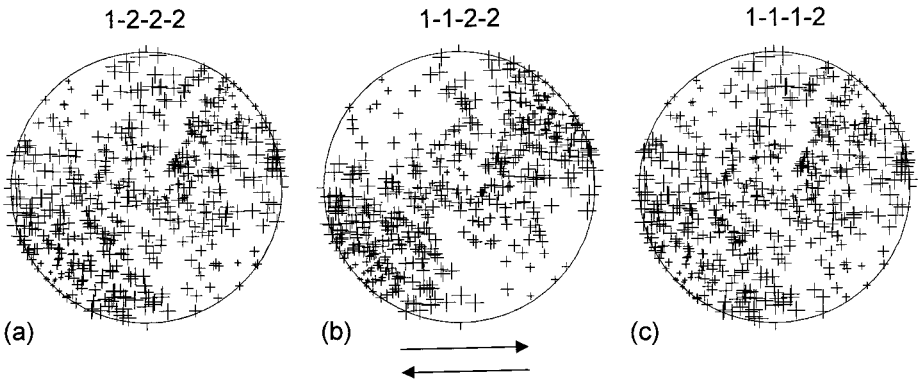


**Figure 5.** Equivalent strain rate in grains represented by symbol size on [100] pole figures for critical shear stress sets (a) 1-2-2-2, (2)1-1-2-2, and (c) 1-1-1-1 (Table 1). There are 200 grains after 40% equivalent shear deformation.

**Table 2.** Recrystallization Parameters

| | Definition | Nucleation Model | Growth Model |
|---|---|---|---|
| $C$ | growth velocity | 800 | 50 |
| $C_{min}$ | minimum size | 10% | 10% |
| $B_1$ | nucleation threshold | 75% | 95% |
| $B_2$ | nucleus size | 15% | 15% |
| $B_3$ | transfer size | 80% | 80% |

diagonal directions, particularly in the directions of the asymmetric texture maximum $A$. Those grains barely deform. Highest strain rates are for orientations near the N-S poles and E-W points. For clarification, it should be stated that a pole figure representation is incomplete for orientation parameters. It is possible to have soft and hard [100] symbols close together, e.g., in the center of the pole figures, depending on the full crystallographic orientation.

From such representations we can qualitatively estimate what may happen during dynamic recrystallization. If growth is prevalent, we expect orientations with small symbols (hard and therefore fewer dislocations and less stored energy) to grow at the expense of softer grains with higher stored energy and to dominate the recrystallization texture. Such a texture is likely to be similar to the deformation texture because the hard grains coincide with the texture maximum. If nucleation dominates, orientations with large symbols (higher stored energy) will prevail, and the texture may be quite different.

In the model we allow for dynamic recrystallization beginning after 20 deformation steps of 2.0% (equivalent strain $\varepsilon_{vm} = 0.4$, shear $\gamma = 0.68$). Recrystallization parameters are given in Table 2. The texture evolution is illustrated with [100] and [010] pole figures with symbols illustrating growth and nucleation (Figures 6 and 7.) Soft orientations nucleate (crosses), whereas hard orientations grow (increasing size of pluses). Grains that have vanished during the last step are indicated by diamonds. Out of many simulations we only illustrate one growth-dominated case (Figure 6) and one nucleation-dominated case (Figure 7), each for 1-2-2-2- and 1-1-1-2 critical shear stress ratios.

The simulations for growth are as expected. In this case the pole figure is quickly depleted of soft orientations, and orientations in the asymmetric (30°) maximum have an advantage and grow (Figure 6). A few orientations nucleate but cannot compete and ultimately disappear. In this case a very strong texture develops that is similar to the deformation texture but much sharper. All three sets of critical shear stress models give similar results. Implicit in the growth model is that ultimately only one orientation survives.

In the nucleation-dominated case, grains that are intermediate in plastic strength disappear first (Figure 7). Hard orientations in the position of the asymmetric deformation texture maximum $A$ grow. Many soft orientations nucleate, largely in two main concentrations, one with [100] near the shear direction (component $B$) and a second asymmetric one at high angles to the slip direction (component $C$). In the next strain steps, nuclei have an advantage over relatively hard original grains because their critical shear stresses (and so their stored energies) have been reset. The size of nucleated grains increases, and harder grains that have not nucleated disappear (diamonds) because their residual strain energies are still higher than those of new nuclei. After 55 steps all old grains have disappeared. The nucleated grains at high angles (component $C$) rotate with the sense of shear toward the 30° orientation (component $A$) and slowly disappear. The soft orientations near the shear direction (component $B$) concentrate, grow, and nucleate several times. After 80 steps ($\varepsilon_{vm} = 1.6$, $\gamma = 2.7$) those latter orientations which represent the easy slip orientation for (010)[100] slip dominate the texture.

In the simulation the transition from a deformation to a recrystallization texture is quite rapid, and once the easy slip recrystallization texture has been established, it does not change during further straining. In the model the deformation texture (component $A$) transforms at intermediate strains to a bimodal texture (components $B$ and $C$) and ultimately stabilizes in a single component (component $B$) during dynamic recrystallization. Even though assumed critical shear stress ratios 1-2-2-2 and 1-1-1-2 are quite different, the texture evolution in both cases is rather similar.

For easier comparison with experiments we have also prepared contoured pole figures (at 20 steps for deformation and 75 steps after nucleation dominated dynamic recrystallization). This was done by entering individual orientations into discrete orientation distribution cells, smoothing with a 15° Gauss filter and recalculating pole figures (all with the software BEARTEX [*Wenk et al*., 1998]). Figure 8 confirms the similarity of the simulated deformation texture with that from the experiments of *Zhang and Karato* [1995] (Figure 1a) and also illustrates a close similarity of the experimental and simulated recrystallization texture (Figure 1b).

In order to better understand the behavior during deformation and recrystallization we illustrate the rotation trajectory of four individual grains on [100] pole figures (Figure 9). The first grain (Figure 9a) is initially in the easy slip orientation, i.e., slip plane and slip direction coincide with the shear plane and shear direction, respectively, for the dominant slip system (010)[100]. The second grain (Figure 9b) is perpendicular to it, i.e., shear plane and shear direction exchanged. Since the stress is a symmetric tensor, both grains are initially subject to the same stress and are in an optimal orientation for simple shear deformation (assuming again that (010)[100] slip is active). Both grains rotate toward the 30° texture maximum. The first grain (Figure 9a) nucleates due to a high incremental strain, then reverses its path and increases in size, the second grain (Figure 9b) does not nucleate and disappears. The third and fourth grains (Figures 9c and 9d, respectively) are two that ultimately (after dynamic recrystallization) end up in the easy slip orientation. One of them was initially close to that orientation (Figure 9d) and the other underwent larger rotations (Figure 9c). It should be noted that all orientations that end up in component $B$ were already initially in the vicinity and have not undergone large rotations.

During the deformation stage an average number of 3–4 slip systems are active in each grain (a system is counted as active if it contributes more than 5% to the overall strain) and strain is distributed over all 4 systems (Figure 10). However, most of the shear is on the (010)[100] system. The texture evolution and slip system activity is also reflected in the flow stress; during deformation the systems harden and the flow stress increases, but during nucleation-dominated recrystallization and with increasing importance of the easy slip component $B$, there is geometric softening, reaching a steady state (Figure 11).

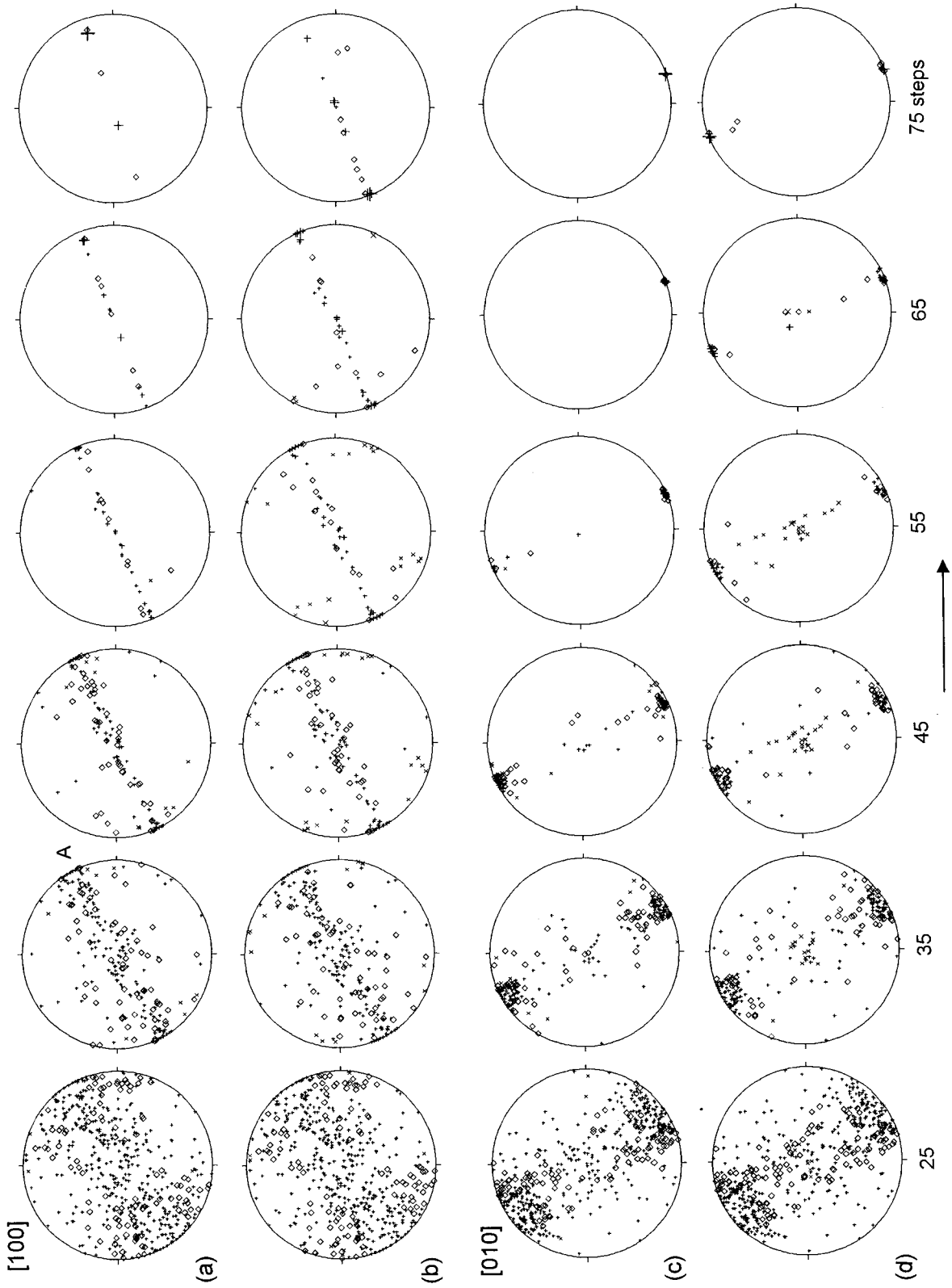


**Figure 6.** Texture evolution during dynamic recrystallization dominated by growth for sets (a,c) 1-2-2-2 and (b,d) 1-1-1-2 for the [100] and [010] pole figures. Symbol size is proportional to grain volume, pluses are parent grains, crosses are grains that have nucleated at least once, and diamonds are grains that have disappeared during the last step. Projections are equal-area.

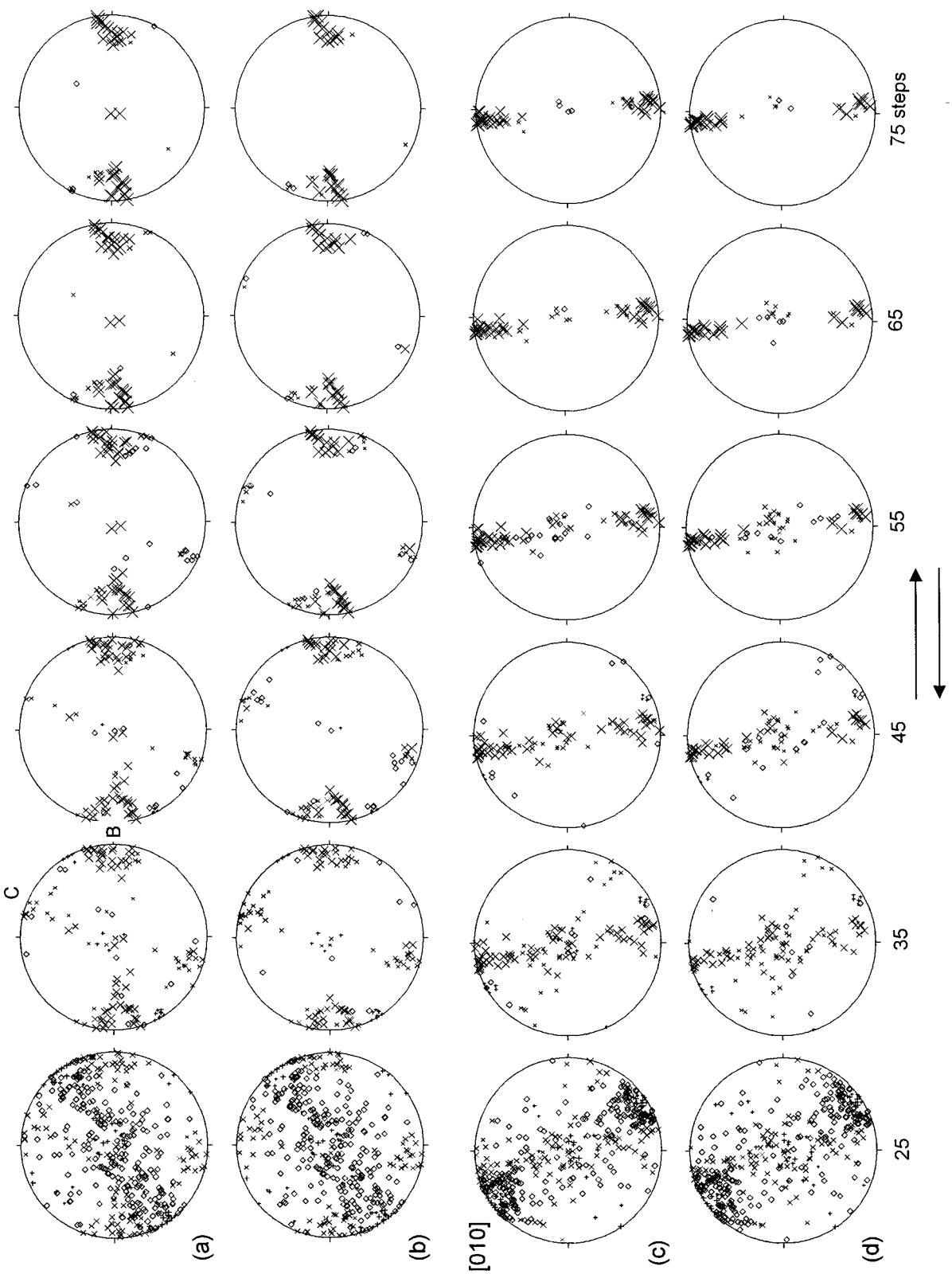


**Figure 7.** Texture evolution during dynamic recrystallization with dominating nucleation for sets (a,c) 1-2-2-2 and (b,d) 1-1-1-2 for [100] and [010] pole figures. Symbol size is proportional to grain volume, pluses are parent grains, crosses are grains that have nucleated at least once, and diamonds are grains that have disappeared during the last step. Projections are equal-area.

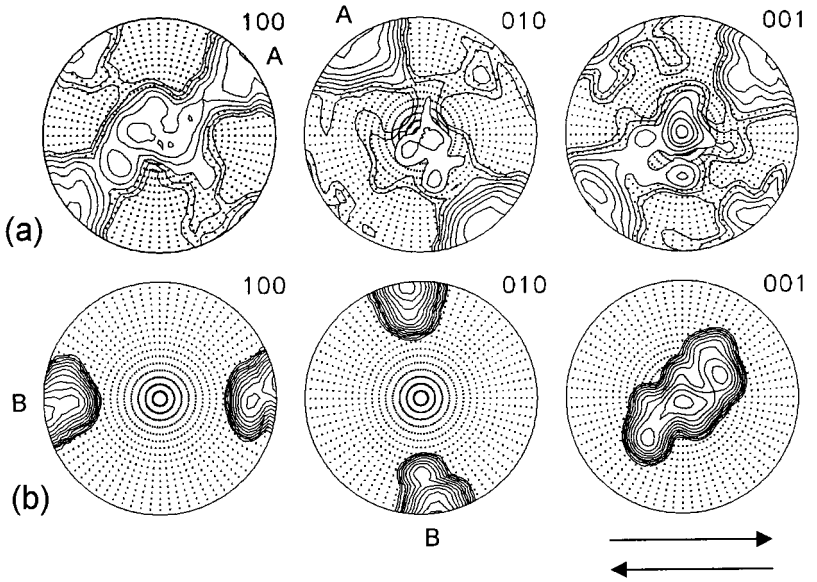


**Figure 8.** Contoured pole figures corresponding to set 1-1-2-2. For (a) deformation $\gamma = 0.4$ (20 steps) and (b) nucleation-dominated recrystallization after $\gamma = 1.5$ (75 steps). Individual orientations have been smoothed with a 15° Gauss filter. Projections are equal-area; logarithmic contours are 0.5, 0.7, 1.0, 1.4, 2 m.r.d., etc.; dot pattern is below 1 m.r.d. Compare with the experimental data in Figure 1.

## 4. Discussion

The present polycrystal plasticity simulations of olivine deformed by slip in simple shear geometry are largely consistent with previous modeling results which all predicted the development of an asymmetric deformation texture (component $A$). This texture is fairly insensitive to the exact values for the critical resolved shear stresses on the various systems and to hardening coefficients, as long as the slip system (010)[100] is at least equally active as (001)[100] and (100)[001]. From the individual grain rotation trajectories (Figures 9 and 8 of *Wenk et al.* [1991]) we observe different rotation increments for different initial orientations. Rotations are minimal for orientations near the asymmetric texture component $A$.

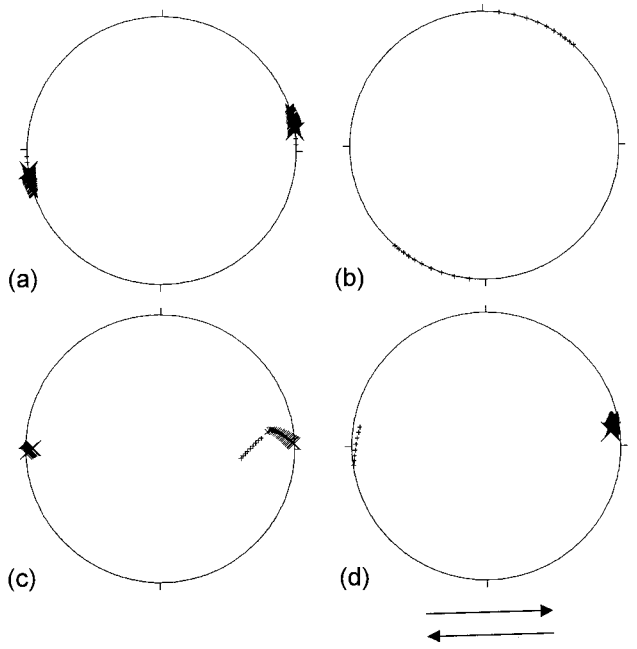


**Figure 9.** The [100] rotation trajectories of four individual grains. Starting orientations are given by dot. Strain increments are 5%. Symbol size is proportional to grain volume.

As the asymmetric deformation texture evolves, crystals become less favorably oriented for slip, and this causes geometric hardening. In addition, slip systems harden due to accumulation of dislocations. Both factors lead in the model to an increase in the flow stress (Figure 11). For very high strains and a strong texture the few slip systems in olivine cannot accommodate the strain in a polycrystal plasticity model, even in a relaxed self-consistent framework, and for numerical stability it is necessary to introduce additional artificial hard slip systems that are not realistic. In the present model where pure deformation only proceeds to a strain of 40%, activation of these systems marked with asterisks in Table 1 is not significant, and at larger strains, recrystallization alleviates incompatibility. However, they were activated in the growth simulations as the hard asymmetric single-component texture was approached. Therefore the sum of activity of slip systems for the four modes in Figure 10 for large strains (beyond 50 steps) is not unity, and the flow stress becomes unrealistically large (Figure 11). This has no physical meaning.

In high-temperature deformation of rocks, diffusive mechanisms such as climb may accommodate strain incompatibilities between grains but are not included in our polycrystal plasticity model. Diffusive mechanisms greatly influence the mechanical behavior but have a much smaller effect on preferred orientation. Therefore we have less confidence in details of the simulated stress-strain curves than in texture patterns. However, the softening and steady state during nucleation recrystallization is realistic as the easy slip orientation is approached.

For nucleation-dominated recrystallization the final texture is the easy slip orientation of the softest slip system. Easy slip is confined to simple shear deformation because it implies that

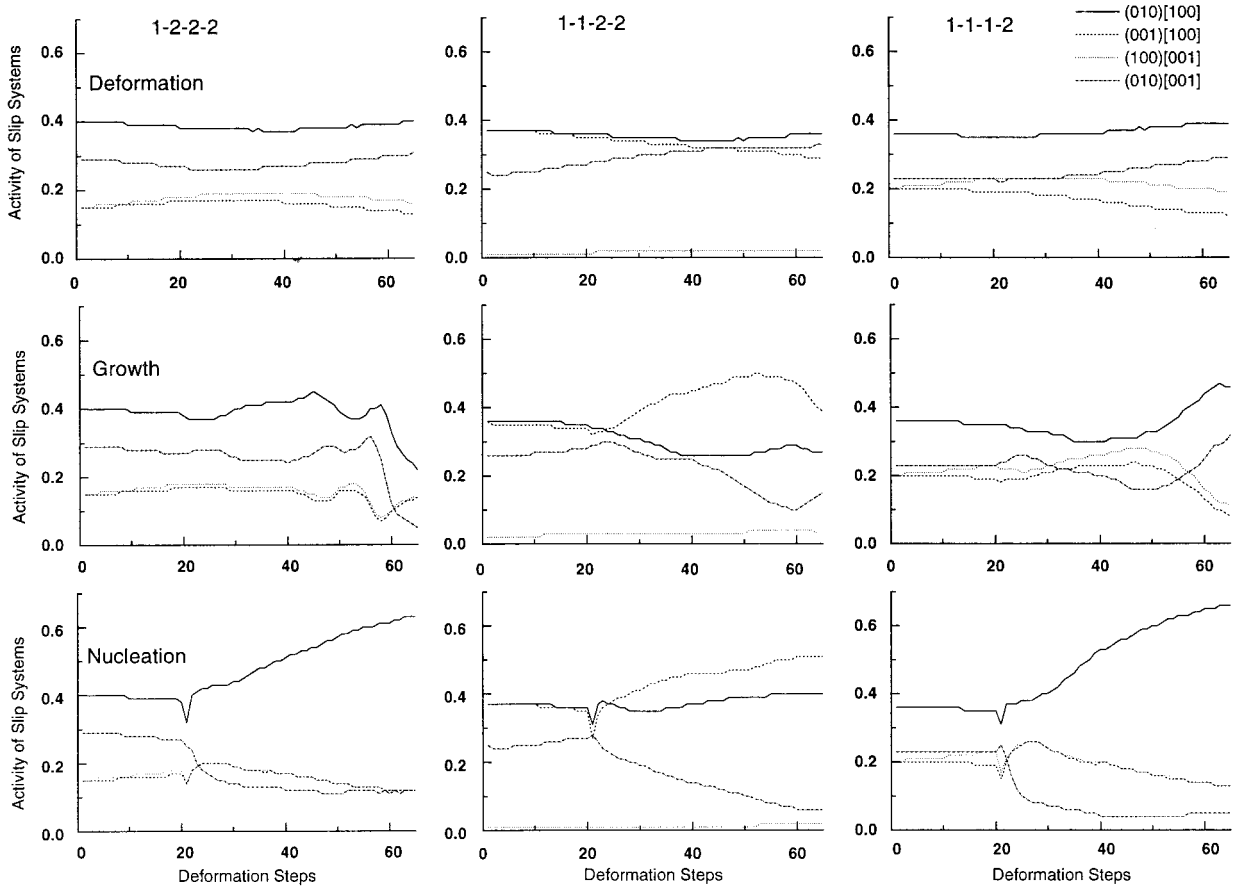


**Figure 10.** Activity of slip systems for models of deformation, growth, and nucleation with different critical shear stress ratios listed in Table 1. The abscissa gives the number of deformation steps.

the microscopic slip direction is parallel to the macroscopic shear direction and the microscopic slip plane is parallel to the macroscopic shear plane. Only for simple shear can a single-slip system accommodate a macroscopic strain. In all other cases, at least two slip systems are needed. If a crystal is in that orientation and is deformed in a Taylor-type framework (homogeneous strain), it will deform on a single-slip system and does not rotate. In a self-consistent framework with a random orientation distribution those crystals will rotate because of overall compatibility with the medium (Figure 8a). However, if all crystals are in easy slip orientations, then in a self-consistent sense those orientations are also stable, which is the reason why these orientations remain during dynamic recrystallization to very large strains. It is as if a microcrystal deforms in a macrocrystal by single slip. In the recrystallization model, nucleation selects these orientations because they correspond to the most highly deformed grains.

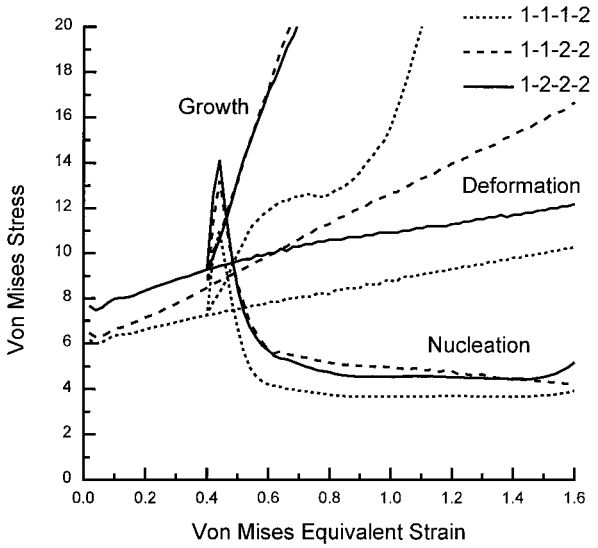


**Figure 11.** Stress-strain curves for models of deformation, growth, and nucleation with different critical shear stress ratios (Table 1).

Easy slip has been documented as a final orientation in several mineral systems investigated experimentally in simple shear. In quartz [*Dell'Angelo and Tullis*, 1989], olivine [*Zhang and Karato*, 1995], ice [*Bouchez and Duval*, 1982; *Burg et al*., 1986], calcite [*Kunze et al*., 1998], and norcamphor [*Herwegh and Handy*, 1996] a single stable texture component developed that can be interpreted as an easy slip orientation of the most active slip system. In all these experiments, rocks are recrystallized by subgrain rotation and with a reduction in grain size, a situation very similar to the case illustrated here.

A major concern has always been how recrystallized grains arrive at this easy slip orientation. From polycrystal plasticity simulations it has been clear that grains could not have rotated into those orientations by slip. The dynamic recrystallization simulations in this study may provide an answer: These very

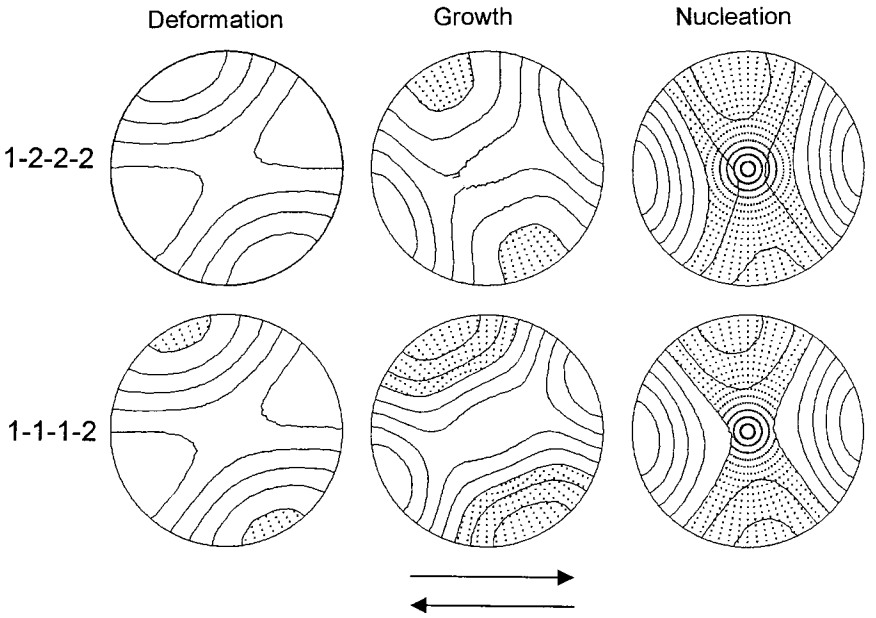


**Figure 12.** Normalized *P* velocity surfaces of olivine polycrystals deformed in simple shear for sets 1-2-2-2 and 1-1-1-2, deformation, growth, and nucleation after $\gamma = 1.2$ (60 steps). Highest velocity is 1000, contour interval is 20 with dot pattern indicating velocities below 900. Projections are equal-area.

special orientations have not rotated much but originated as components of the deformation texture. They represent grains that were most heavily deformed, nucleated repeatedly, and grew. In the model, and for simple shear deformation, other orientations rotate toward component $B$ to minimize compatibility problems in a self-consistent sense, as the easy slip component starts to dominate the texture. In the simulations there is a second component with [100] at high angles to the shear plane ($C$). Contrary to the easy slip component $B$, component $C$ is not stable but with increasing strain its importance diminishes because it also rotates slowly with the sense of shear.

Even though the model has no topologic or size information, the simulations provide some information on microstructures. In the model, as it stands, a uniform initial weight is given to all grains. These weights change during growth and shrinking, but because the model does not consider the grain topology a detailed size evolution during boundary migration is not possible. In a growth-dominated process, starting with a uniform grain size, first a bimodal distribution develops, then the smaller unstable grains disappear, and a few large grains ultimately dominate.

For dominant nucleation the model gives the impression that after recrystallization only a few large grains are left, contrary to the experiment where grain size is reduced [*Zhang and Karato*, 1995, Figure 2b]. This apparent contradiction comes from the fact that in the model we have to keep the total number of grains constant, also counting those that disappeared. With a constant nucleation rate $B_2$, all nuclei are collected in the same orientation and appear as a single point in the pole figures. In reality, each represents many nuclei that may have slightly different orientations. The model also simplifies in assigning the nucleus exactly the same orientation as the host, whereas in reality, nuclei do have misorientations. Therefore the model exaggerates the texture strength.

Textures are related to polycrystal physical properties, and seismologists, concerned with anisotropy in the upper mantle, have been particularly interested in the influence of preferred orientation of olivine on the elastic properties, including the effect of recrystallization. Recrystallization may produce a random orientation pattern with weak anisotropy, but this is rare for strongly deformed materials, and *Ben Ismail and Mainprice* [1998] have shown that most mantle-derived peridotites, with evidence for recrystallization, display strong preferred orientation of olivine. We have explored the effects of the different models (deformation, growth, and nucleation) on the anisotropy of seismic wave propagation. Elastic properties of the simulated aggregates were calculated by averaging single-crystal properties of olivine over all orientations, using an elastic self-consistent model [*Tomé*, 1998]. Next, we calculated *P* wave velocity surfaces for models 1-2-2-2 and 1-1-1-2 simulations to a strain $\alpha = 1.2$ for pure deformation, nucleation, and growth-dominated recrystallization (Figure 12). The *P* velocity surfaces are normalized so that the highest values in all of them are 1000, and in all of them this maximum is near the shear direction. As expected, there is a slight asymmetry relative to the shear plane and shear direction, except for the nucleation-dominated texture, but the overall patterns and magnitudes of anisotropy are similar, 10% for deformation and 15% for recrystallization. So far, models predicting anisotropy due to olivine deformation in the upper mantle relied on deformation by slip only [*Chastel et al.*, 1993; *Dawson and Wenk*, 1999; *Wenk et al.*, 1999], and these models need to be refined to include recrystallization. With these simulation results, the general conclusion still holds that much of the observed seismic anisotropy patterns in the upper mantle [e.g., *Anderson and Dziewonski*, 1982; *Morris et al.*, 1969; *Silver*, 1996] are due to development of preferred orientation during convection. However, the general concept to associate fast velocities with the "flow direction" is misleading and inaccurate: in a heterogeneous convection system the displacement gradient tensor changes along a flow line and the flow direction does not coincide with the shear direction [*Dawson and Wenk*, 1999].

Olivine does not flow along [100] like a log in a stream. Olivine crystals in mantle peridotites are largely equiaxed and recrystallized. They grow in such an orientation that [100] is close to parallel to the shear direction.

## 5. Conclusions

The viscoplastic self-consistent polycrystal plasticity theory, modified to include recrystallization, simulates textural features that have been observed in simple shear experiments on olivine aggregates. Different textures are simulated for deformation, for nucleation-dominated recrystallization, and for growth-dominated (boundary migration) recrystallization. Deformation textures and boundary migration textures are similar, with [100] axes in an asymmetric maximum inclined 20°–30° to the shear direction. For nucleation the main texture component has a [100] maximum parallel to the shear direction, corresponding to a (010)[100] easy slip orientation. As in many geological systems, though this is not universal, it appears that also in simple shear experiments of olivine the most strongly deformed orientation components dominate the recrystallization texture. The components are selected from deformation texture components, depending on the deformation state of different orientations.

While there are distinct differences between deformation and recrystallization textures, the effects on seismic wave propagation appear minor. Particularly, since [100] is the fast direction in single crystals, the simulations suggest that a polycrystal deformed in simple shear will have a fast direction near the shear direction [*Hess*, 1964; *Christensen*, 1984; *Silver*, 1996]. For the nucleation model it is almost perfectly aligned with the shear direction.

In the future, it will be necessary to experimentally determine for olivine the fields of boundary migration recrystallization and subgrain rotation in a similar way as has been done for quartz [*Hirth and Tullis*, 1992]. By comparison of experimental results with textures and microstructures in naturally deformed peridotites of mantle origin the deformation and recrystallization mechanisms of rocks in the upper mantle can be assessed. At that point it will become possible to produce realistic models of texture and anisotropy development in the Earth by including dynamic recrystallization. This contribution is a first step.

**Acknowledgments.** We greatly acknowledge numerous discussions on the enigma of recrystallization with Dave Embury, Olaf Engler, Pierre Guyot, John Hirth, Fred Kocks, Heinz Mecking, and Ichiko Shimizu. Bill Durham was helpful in clarifying issues of olivine deformation. We also appreciate the thoughtful input by N. Christensen, D. Mainprice, and J. Tullis, who reviewed the manuscript. Maureen Montagnat helped with incorporating the new recrystallization model into the VPSC computer code while on an exchange visit supported by the France-Berkeley Fund. S. Zhang made numerical data of his experiments available. H. R. W. was supported by NSF (EAR 94-17580), IGPP-LLNL (98-GS031) (under auspices by DOE contract W-7405-Eng-48), and by UCDRD as an exchange visiting scholar at CMS-LANL.

## References

Anderson, D. L., and A. M. Dziewonski, Upper mantle anisotropy: Evidence from free oscillations, *Geophys. J. R. Astron. Soc*., *69*, 383–404, 1982.

Avé Lallemant, H. G., and N. L. Carter, Syntectonic recrystallization of olivine and modes of flow in the upper mantle, *Geol. Soc. Am. Bull*., *81*, 2203–2220, 1970.

Bai, Q., S. J. Mackwell, and D. L. Kohlstedt, High-temperature creep of olivine single crystals, 1, Mechanical results for buffered samples, *J. Geophys. Res*., *96*, 2441–2463, 1991.

Ben Ismail, W., and D. Mainprice, An olivine fabric database: An overview of upper mantle fabrics and seismic anisotropy, *Tectonophysics*, *296*, 145–158, 1998.

Blackman, D. K., J.-M. Kendall, P. R. Dawson, H.-R. Wenk, D. Boyce, and J. P. Morgan, Teleseismic imaging of subaxial flow at mid-ocean ridges: Travel-time effects of anisotropic mineral texture in the mantle. *Geophys. J. Int*., *127*, 415–426, 1996.

Bouchez, J. L., and P. Duval, The fabric of polycrystalline ice deformed in simple shear: experiments in torsion, natural deformation and geometrical interpretation. *Textures Microstruct*., *5*, 171–190, 1982.

Burg, J. P., C. J. Wilson, and J. C. Mitchell, Dynamic recrystallization and fabric development during simple shear deformation of ice, *J. Struct. Geol*., *8*, 857–870, 1986.

Canova, G. R., H.-R. Wenk, and A. Molinari, Simulation of texture development in polyphase materials, *Acta Metall. Mater*., *40*, 1519–1530, 1992.

Chastel, Y. B., P. R. Dawson, H.-R. Wenk, and K. Bennett, Anisotropic convection with implications for the upper mantle. *J. Geophys. Res*., *98*, 17,757–17,771, 1993.

Christensen, N. I., The magnitude, symmetry, and origin of upper mantle anisotropy based on fabric analyses of ultramafic tectonites, *Geophys. J. R. Astron. Soc*., *76*, 89–111, 1984.

Dawson, P. R., and A. J. Beaudoin, Finite element modeling of heterogeneous plasticity, in *Texture and Anisotropy. Preferred Orientations in Polycrystals and Their Effect on Materials Properties*, edited by U. F. Kocks, C. Tomé, and H.-R. Wenk, pp. 512–531, Cambridge Univ. Press, New York, 1998.

Dawson, P. R., and H.-R. Wenk, Anisotropy development in the upper mantle based on polycrystal plasticity, *Philos. Mag. A*, in press, 1999.

Dell'Angelo, L. N., and J. Tullis, Fabric development in experimentally sheared quartzites, *Tectonophysics*, *169*, 1–21, 1989.

Doherty, R. D., Recrystallization and texture, *Prog. Mater. Sci*., *42*, 39–58, 1997.

Drury, M. R., and J. L. Urai, Deformation-related recrystallization processes, *Tectonophysics*, *172*, 235–253, 1990.

Duval, P., Creep and fabrics of polycrystalline ice under shear and compression, *J. Glaciol*., *27*, 129–140, 1981.

Engler, O., Nucleation and growth during recrystallisation of aluminium alloys investigated by local texture analysis, *Mater. Sci. Technol*., *12*, 859–872, 1996.

Eshelby, J., The determination of the elastic field of an ellipsoidal inclusion, and related problems, *Proc. R. Soc. London Ser. A*, *241*, 376–396, 1957.

Guillopé, M., and J.-P. Poirier, Dynamic recrystallization during creep of single-crystalline halite: An experimental study, *J. Geophys. Res*., *84*, 5557–5567, 1979.

Haessner, F., *Recrystallization of Metallic Materials*, Riederer, Stuttgart, Germany, 1978.

Hanson, D. R., and H. A. Spetzler, Transient creep in natural and synthetic, iron-bearing olivine single crystals: Mechanical results and dislocation microstructures, *Tectonophysics*, *235*, 293–315, 1994.

Herwegh, M., and M. Handy, The evolution of high temperature mylonitic microfabrics: Evidence from simple shearing of a quartz analogue (norcamphor), *J. Struct. Geol*., *18*, 689–710, 1996.

Hess, H. H., Seismic anisotropy of the uppermost mantle under oceans, *Nature*, *203*, 629–631, 1964.

Hirth, G., and J. Tullis, Dislocation creep regimes in quartz aggregates, *J. Struct. Geol*., *14*, 145–159, 1992.

Hirth, J. P., and J. Lothe, *Theory of Dislocations*, McGraw-Hill, New York, 1982.

Humphreys, F. J., and M. Hatherly, *Recrystallization and Related Annealing Phenomena*, Oxford Univ. Press, New York, 1995.

Jessell, M. W., Simulation of fabric development in recrystallizing aggregates, I, Description of the model, *J. Struct. Geol*., *10*, 771–778, 1988.

Karato, S., The role of recrystallization in the preferred orientation of olivine, *Phys. Earth Planet. Inter*., *51*, 107–122, 1988.

Karato, S., and K.-H. Lee, Stress-strain distribution in deformed olivine aggregates: Inference from microstructural observations and implications for texture development, in *Proceedings of the 12th International Conference on Textures of Materials*, edited by J. A. Szpunar, pp. 1546–1555, Natl. Res. Counc. Res. Press, Ottawa, Canada, 1999.

Karato, S., M. I. Toriumi, and T. Fujii, Dynamic recrystallization of olivine during high temperature creep, *Geophys. Res. Lett*., *7*, 649–652, 1980.

Kocks, U. F., Laws for work-hardening and low-temperature creep, *J. Eng. Mater. Technol*., *98*, 76–85, 1976.

Kocks, U. F., Kinematics and kinetics of plasticity, in *Texture and Anisotropy: Preferred Orientations in Polycrystals and Their Effect on Materials Properties*, edited by U. F. Kocks, C. Tomé, and H.-R. Wenk, pp. 326–389, Cambridge Univ. Press, New York, 1998.

Kohlstedt, D. L., and C. Goetze, Low-stress high-temperature creep in olivine single crystals, *J. Geophys. Res*., *79*, 2045–2051, 1974.

Kunze, K., M. Pieri, L. Burlini, and H.-R. Wenk, Texture development in calcite during deformation and recrystallization: Numerical simulations of high strain torsion experiments, *Eos Trans. AGU*, *79*(45), Fall Meet. Suppl., F851, 1998.

Lebensohn, R. A., and C. N. Tomé, A self-consistent anisotropic approach for the simulation of plastic deformation and texture development of polycrystals—Application to zirconium alloys, *Acta Metall. Mater*., *41*, 2611–2624, 1993.

Lebensohn, R. A., and C. N. Tomé, A self-consistent visco-plastic model: Prediction of rolling textures of anisotropic polycrystals, *Mater. Sci. Eng. A*, *175*, 71–82, 1994.

Lebensohn, R. A., H.-R. Wenk, and C. N. Tomé, Modelling deformation and recrystallization textures in calcite, *Acta Mater*., *46*, 2683–2693, 1998.

Loretto, M. H., L. M. Clarebrough, and R. L. Segall, The stacking-fault energy of silver, *Philos. Mag*., *10*, 731–733, 1964.

Loretto, M. H., L. M. Clarebrough, and R. L. Segall, Stacking-fault tetrahedra in deformed face-centered cubic metals, *Philos. Mag*., *11*, 459–465, 1965.

Mercier, J. C. C., Olivine and pyroxenes, in *Preferred Orientation in Deformed Metals and Rocks: An Introduction to Modern Texture Analysis*, edited by H.-R. Wenk, pp. 407–430, Academic, San Diego, Calif., 1985.

Molinari, A., G. R. Canova, and S. Ahzi, A self-consistent approach of the large deformation polycrystal viscoplasticity, *Acta Metall*., *35*, 2983–2994, 1987.

Morris, G. B., R. W. Raitt, and G. G. Shor, Velocity anisotropy and delay time maps of the mantle near Hawaii, *J. Geophys. Res*., *74*, 4300–4316, 1969.

Nicolas, A., F. Boudier, and A.-M. Boullier, Mechanisms of flow in naturally and experimentally deformed peridotites, *Am. J. Sci*., *273*, 853–876, 1973.

Nicolas, J. L., F. Bouchez, and J. C. Mercier, Textures, structures and fabrics due to solid state flow in some European lherzolites, *Tectonophysics*, *12*, 55–86, 1971.

Parks, D. M., and S. Ahzi, Polycrystalline plastic deformation and texture evolution for crystals lacking five independent slip systems, *J. Mech. Phys. Solids*, *38*, 701–724, 1990.

Pieri, M., and D. L. Olgaard, High shear deformation of Carrara marble: Rheological and microstructural results from torsion experiments, *Eos Trans. AGU*, *78*(46), Fall Meet. Suppl., F723, 1997.

Poirier, J. P., and M. Guillopé, Deformation induced recrystallization of minerals, *Bull. Mineral*., *102*, 67–74, 1979.

Sachs, G., Zur Ableitung einer Fliessbedingung, *VDI Z*., *72*, 734–736, 1928.

Schmid, S. M., and M. Casey, Complete fabric analysis of some commonly observed quartz *x*-axis patterns, in *Mineral and Rock Deformation: Laboratory Studies—The Patterson Volume*, *Geophys. Monogr. Ser*., vol. 36, edited by B. E. Hobbs and H. C. Heard, pp. 263–286, AGU, Washington, D. C., 1986.

Silver, P. G., Seismic anisotropy beneath the continents: Probing the depths of geology, *Annu. Rev. Earth Planet. Sci*., *24*, 385–432, 1996.

Skrotzki, W., A. Wedel, K. Weber, and W. F. Müller, Microstructure and texture in lherzolites of the Balmuccia massif and their significance regarding the thermomechanical history, *Tectonophysics*, *179*, 227–251, 1990.

Solas, D. E., C. T. Tomé, O. Engler, and H.-R. Wenk, A coupled Monte-Carlo and N-site self-consistent approach to model static recrystallization, in *The 4th International Conference on Recrystallization and Related Phenomena*, edited by T. Sakai and H. G. Suzuki, pp. 639–644, Jpn. Inst. of Metals, Tokyo, 1999.

Stocker, R. L., and M. F. Ashby, On the rheology of the upper mantle, *Rev. Geophys*., *11*, 391–426, 1973.

Takeshita, T., H.-R. Wenk, G. Canova, and A. Molinari, Simulation of dislocation-assisted plastic deformation in olivine polycrystals, in *Deformation Processes in Minerals, Ceramics and Rocks*, edited by D. J. Barber and P. G. Meredith, pp. 365–377, Unwin Hyman, Boston, Mass., 1990.

Takeshita, T., H.-R. Wenk, and R. Lebensohn, Development of preferred orientation and microstructure in sheared quartzite: Comparison of natural and simulated data, *Tectonophysics*, in press, 1999.

Taylor, G. I., Plastic strain in metals, *J. Inst. Metals*, *62*, 307–324, 1938.

Tomé, C. N., Tensor properties of textured polycrystals, in *Texture and Anisotropy. Preferred Orientations in Polycrystals and Their Effect on Materials Properties*, edited by U. F. Kocks, C. Tomé, and H.-R. Wenk, pp. 550–595, Cambridge Univ. Press, New York, 1998.

Tomé, C. N., and G. R. Canova, Self-consistent modeling of heterogeneous plasticity, in *Texture and Anisotropy. Preferred Orientations in Polycrystals and Their Effect on Materials Properties*, edited by U. F. Kocks, C. Tomé, and H.-R. Wenk, pp. 466–510, Cambridge Univ. Press, New York, 1998.

Tommasi, A., A. Vauchez, D. Mainprice, R. Russo, and G. Canova, Forward modeling of the development of seismic anisotropy in ocean basins through resistive drag of sublithospheric mantle, *Eos Trans. AGU*, *78*(46), Fall Meet. Suppl., F18, 1997.

Toriumi, M., and S. Karato, Preferred orientation development of dynamically recrystallized olivine during high temperature creep, *J. Geol*., *93*, 407–417, 1985.

Urai, J. L., W. D. Means, and G. S. Lister, Dynamic recrystallization of minerals, in *Mineral and Rock Deformation: Laboratory Studies—The Paterson Volume Geophys. Monogr. Ser*., vol. 36, edited by B. E. Hobbs and H. C. Heard, pp. 161–199, AGU, Washington, D. C., 1986.

Wenk, H.-R., Plasticity modeling in minerals and rocks, in *Texture and Anisotropy: Preferred Orientations in Polycrystals and Their Effects on Materials Properties*, edited by U. F. Kocks, C. Tomé, and H.-R. Wenk, pp. 550–595, Cambridge Univ. Press, New York, 1998.

Wenk, H.-R., A voyage through the deformed Earth with the self-consistent model, *Model. Simulat. Mater. Sci. Eng*., *7*, in press, 1999.

Wenk, H.-R., T. Takeshita, E. Bechler, B. G. Erskine, and S. Matthies, Pure shear and simple shear calcite textures: Comparison of experimental, theoretical and natural data, *J. Struct. Geol*., *9*, 731–745, 1987.

Wenk, H.-R., G. Canova, A. Molinari, and U. F. Kocks, Viscoplastic modeling of texture development in quartzite, *J. Geophys. Res*., *94*, 17,895–17,906, 1989.

Wenk, H.-R., K. Bennett, G. Canova, and A. Molinari, Modelling plastic deformation of peridotite with the self-consistent theory, *J. Geophys. Res*., *96*, 8337–8349, 1991.

Wenk, H.-R., G. Canova, Y. Brechet, and L. Flandin, A deformation-based model for recrystallization, *Acta Mater*., *45*, 3283–3296, 1997.

Wenk, H.-R., S., Matthies, J. Donovan, and D. Chateigner, BEARTEX, a Windows-based program system for quantitative texture analysis, *J. Appl. Crystallogr*., *31*, 262–269, 1998.

Wenk, H.-R., P. Dawson, C. Pelkie, and Y. Chastel, Texturing of rocks in the Earth's mantle: A convection model based on polycrystal plasticity, video, AGU, Washington, D.C., in production, 1999.

Zhang, S., and S.-Y. Karato, Lattice preferred orientation of olivine aggregates deformed in simple shear, *Nature*, *375*, 774–777, 1995.

C. N. Tomé, Materials, Science and Technology Division, Los Alamos National Laboratory, MST-8, MS G755, Los Alamos, NM 87545. (tome@lanl.gov)

H.-R. Wenk, Department of Geology and Geophysics, University of California, Berkeley, CA 94720-4767. (wenk@seismo.berkeley.edu)

(Received December 1, 1998; revised May 27, 1999;
accepted July 20, 1999.)